

INVITED ARTICLE

Gaussian approximation to single particle correlations at and below the picosecond scale for Lennard-Jones and nanoparticle fluids

Ramses van Zon^{1,3}, S S Ashwin^{2,3} and E G D Cohen³

¹ Chemical Physics Theory Group, Department of Chemistry, University of Toronto, 80 St George Street, Toronto, Ontario M5S 3H6, Canada

² Department of Chemistry, University of Saskatchewan, 110 Science Place, Saskatoon, Saskatchewan S7N 5C9, Canada

³ The Rockefeller University, 1230 York Avenue, New York, NY, 10065-6399, USA

E-mail: rzon@chem.utoronto.ca

Received 31 January 2007

Published 4 April 2008

Online at stacks.iop.org/Non/21/R119

Recommended by J R Dorfman

Abstract

To describe short time (picosecond) and small scale (nanometre) transport in fluids, a Green's function approach was recently developed. This approach relies on an expansion of the distribution of single particle displacements around a Gaussian function, yielding an infinite series of correction terms. Applying a recent theorem (van Zon and Cohen 2006 *J. Stat. Phys.* **123** 1–37) shows that for sufficiently small times the terms in this series become successively smaller, so that truncating the series near or at the Gaussian level might provide a good approximation. In this paper, we derive a theoretical estimate for the time scale at which truncating the series at or near the Gaussian level could be supposed to be accurate for equilibrium nanoscale systems. In order to numerically estimate this time scale, the coefficients for the first few terms in the series are determined in computer simulations for a Lennard-Jones (LJ) fluid, an isotopic LJ mixture and a suspension of a LJ-based model of nanoparticles in a LJ fluid. The results suggest that for LJ fluids an expansion around a Gaussian is accurate at time scales up to a picosecond, while for nanoparticles in suspension (a nanofluid), the characteristic time scale up to which the Gaussian is accurate becomes of the order of 5–10 ps.

PACS numbers: 05.20.-y, 02.30.Mv, 02.60.Cb, 61.20.Ja, 05.60.Cd

(Some figures in this article are in colour only in the electronic version)

1. Introduction

Small clusters of particles suspended in a fluid occur in many forms, from nanoparticles [1–3], quantum dots [4] and colloidal suspensions [5] to biomolecules such as globular proteins [6,7]. Such nanoclusters have a variety of applications, from material coatings to drug delivery by hollow clusters. Both the individual behaviour of nanosized particles [9–11] and their collective behaviour, such as the increased heat conductance in dilute suspensions of nanoparticles (so-called nanofluids) [1], have attracted considerable attention [8].

For the purpose of studying small length scale and short time classical transport phenomena which occur in nanosystems, a Green's function approach was introduced by Kincaid [12]. This approach has the promise of being able, in principle, to describe transport phenomena on all time and length scales, unlike hydrodynamics. The main idea of the theory is to describe the evolution of fluid properties such as its energy, momentum and number density in terms of Green's functions. The application of these Green's functions to nanosystems and systems where time scales at picoseconds or less are important has been an area of some interest [13–16]. In these cases, the Green's functions were expanded around a Gaussian distribution plus an infinite series of corrections, the finite truncation of which yielded excellent agreement with simulations. Even just the Gaussian itself was found to be a reasonable approximation to the Green's functions. An explanation for this could be that the series of corrections has fast convergence, but at that point, it was not known why this could be the case. Since the Gaussian description is much simpler than the full Green's function, one would like to know when fast convergence occurs and when taking the Gaussian approximation suffices. A preliminary answer to this question was found in [17], namely, that for the motion of a single particle in an equilibrium pure Lennard-Jones (LJ) fluid, the Gaussian approximation can be used up to time scales of the order of a picosecond.

One of the applications of the Green's function approach is mass transport in liquids and liquid mixtures. For this case, the Green's functions are essentially the probability distribution functions of displacements (in a time t) of single particles of different components [16]. Thus it is not too surprising that the Green's functions can be expressed in terms of the cumulants of this distribution. These cumulants measure the correlations of the displacement of a single particle; in particular, they measure the departure of the correlations from Gaussian behaviour. As discussed in more detail below, a recent theorem regarding these cumulants implies that when the Green's functions are expanded around a Gaussian distribution, the correction terms to the Gaussian term are proportional to increasing powers of t for short (initial) times t [18]. Analytic expressions for the coefficients in front of the powers of t were also derived in [18]. The values of the first two numerical coefficients are here of particular interest, because they can be computed numerically and, as shown in section 5.2, can then be used to find estimates of the physical time scales below which the expansion of the Green's function around the Gaussian term yields useful results, as appeared to be the case in [12–15]. Numerical values for these coefficients are presented in this paper for various equilibrium LJ-based systems, including nanoparticles in a suspension of LJ particles. We present the resulting orders of magnitude of the relevant time scales on which the first few terms in the series decrease. Non-equilibrium systems will be studied in a future work.

2. Systems

Three systems were studied, namely, a pure LJ fluid, an isotopic binary mixture of LJ particles (in which context the study of short time displacements arose [16]) and a suspension of nanoparticles in a LJ fluid.

In the isotopic binary LJ mixtures, there are N_A particles of mass m_A and N_B particles of mass m_B in a box of size L^3 , such that the number density is $\rho = (N_A + N_B)/L^3$. For the pure LJ fluid, one sets $N_B = 0$. The positions and velocities of the particles will be denoted by $\mathbf{r}_{\lambda i}$ and $\mathbf{v}_{\lambda i}$, respectively, where $\lambda = A$ or B and i is a particle index, which runs from 1 to N_A if $\lambda = A$ and from 1 to N_B if $\lambda = B$. By definition, in an isotopic mixture all pair interaction potentials are the same for all components, but their masses are different. The inter-atomic potential between the particles is the LJ potential

$$V_{AA}(r) = V_{AB}(r) = V_{BB}(r) = 4\epsilon \left[\left(\frac{\sigma}{r} \right)^{12} - \left(\frac{\sigma}{r} \right)^6 \right], \quad (1)$$

where r is the distance between two particles and σ and ϵ are the same for all pairs of particles.

All quantities reported are in LJ units: length in units of σ , temperature in units of ϵ/k_B , density (ρ) in units of σ^{-3} and time in units of $\tau_{LJ} = (\sigma^2 m_A / \epsilon)^{1/2}$, where m_A is the mass of an A -particle. In other words, we will use units in which $\sigma = 1$, $k_B = 1$, $\epsilon = 1$ and $m_A = 1$. Although these are arbitrary units, to understand the physical consequences of our results, we use the LJ parameters of argon as a reference. In this case, one unit of time corresponds to $\tau_{LJ} = 2.16 \times 10^{-12}$ s, while one unit of length corresponds to $\sigma = 0.34$ nm [19, 20].

As mentioned above, apart from the pure LJ fluid and the isotopic binary LJ fluid mixture, a third system which will be studied, namely, a suspension of nanosized particles in a fluid, often called a nanofluid. One can obtain this system from the binary isotopic LJ fluid mixture by changing the B particles to much larger, nanosized particles while the A particles remain regular LJ particles and changing the potentials V_{AB} and V_{BB} in the following way. Each nanoparticle is represented as a spherical cluster of radius R with a smoothed uniform distribution of M LJ particles as proposed in [9] and [21]. Since we are only after typical time scales for which the expansion presented in section 3 is valid, we restrict ourselves here to this simple nanoparticle model. For simplicity, we therefore take the strength of the LJ potential between the constituent LJ particles of the nanoparticles and the fluid particles to be the same, and the mass of the constituent LJ particles of the nanoparticle is also taken to be equal to that of the fluid particles. R will range from 1 to 6 in LJ units, i.e. from 0.34 to 2 nm (which is a typical size of a quantum dot [4]), while M will be chosen such that for $R = 0$, the nanoparticle reduces to a single LJ particle ($M = 1$) while for large R the density of LJ particles within the nanoparticle approaches one. This can be accomplished by choosing M to be $1 + R^3$, leading to a maximum mass ratio of 217 between the nanoparticles and the fluid LJ particles. One can show that the result of integrating the LJ potentials corresponding to all the points in the spherical nanoparticle is that a nanoparticle interacts with a fluid LJ particle through the potential [9, 21]

$$V_{AB}(r) = 4M \left[\frac{\frac{4}{3}R^6 + \frac{36}{5}R^2r^4}{(r^2 - R^2)^9} + \frac{1}{(r^2 - R^2)^6} - \frac{1}{(r^2 - R^2)^3} \right], \quad (2)$$

where r is the distance between the centre of the nanoparticle and the LJ fluid particle, while the interaction potential between two nanoparticles is given by [21]

$$V_{BB}(r) = 4M^2 \left[\frac{r^{10} - \frac{8}{5}R^2r^8 + \frac{216}{25}R^4r^6 - \frac{1504}{75}R^6r^4 + \frac{13696}{525}R^8r^2 - \frac{512}{35}R^{10}}{r^8(r^2 - 4R^2)^7} - \frac{3}{8R^4} \left\{ \frac{r^2 - 2R^2}{r^2(r^2 - 4R^2)} - \frac{1}{4R^2} \ln \left(1 - \frac{4R^2}{r^2} \right) \right\} \right], \quad (3)$$

where r is the distance between the centres of the nanoparticles. Note that because of the much larger size of the nanoparticles, far fewer will fit into a system of given volume than B particles fit in an isotopic LJ mixture of only LJ particles.

The systems studied in this paper are all in canonical equilibrium, i.e. their distribution function $\rho_{\text{eq}}(\Gamma)$ in phase space ($\Gamma = \{\mathbf{r}_{\lambda i}, \mathbf{v}_{\lambda i}\}$) is given by

$$\rho_{\text{eq}}(\Gamma) = e^{-H(\Gamma)/T} / Z, \quad (4)$$

where $Z = \int \exp[-H(\Gamma)/T] d\Gamma$ is the partition function, T is the temperature and H is the Hamiltonian which is of the form

$$H(\Gamma) = \sum_{\lambda=A,B} \sum_{j=1}^{N_\lambda} \frac{m_\lambda |\mathbf{v}_{\lambda j}|^2}{2} + U, \quad (5)$$

where U is a sum of pair potentials:

$$U = \sum_{\lambda=A,B} \sum_{i=1}^{N_\lambda} \sum_{\mu=A,B} \sum_{j=1}^{N_\mu} \frac{1}{2} V_{\lambda\mu}(|\mathbf{r}_{\lambda i} - \mathbf{r}_{\mu j}|), \quad (6)$$

where the prime excludes equal particles (i.e. $\lambda = \mu$ and $i = j$) and the $V_{\lambda\mu}$ are of the form given in (1)–(3). Finally, we remark that the equations of motions are given by

$$\dot{\mathbf{r}}_{\lambda i} = \mathbf{v}_{\lambda i}; \quad \dot{\mathbf{v}}_{\lambda i} = -\frac{1}{m_\lambda} \frac{\partial U}{\partial \mathbf{r}_{\lambda i}}. \quad (7)$$

3. Green's functions and cumulants

We now briefly review the Green's functions approach and its connection with the distribution of single particle displacements. For mass transport processes, the number density $n_\lambda(\mathbf{r}, t)$ of a specific component λ at position \mathbf{r} at time t can be written as

$$n_\lambda(\mathbf{r}, t) = \int d\mathbf{r}' G_\lambda(\mathbf{r} - \mathbf{r}', \mathbf{r}', t) n_\lambda(\mathbf{r}', 0), \quad (8)$$

where $G_\lambda(\mathbf{r}, \mathbf{r}', t)$ is the Green's function for component λ (A or B for a binary mixture), which is defined as [12, 16]

$$G_\lambda(\mathbf{r}, \mathbf{r}', t) = \frac{\langle \delta[\mathbf{r}' + \mathbf{r} - \mathbf{r}_{\lambda i}(t)] \delta[\mathbf{r}' - \mathbf{r}_{\lambda i}(0)] \rangle_{\text{is}}}{\langle \delta[\mathbf{r}' - \mathbf{r}_{\lambda i}(0)] \rangle_{\text{is}}}, \quad (9)$$

where $\mathbf{r}_{\lambda i}(t)$ is the position of the i th particle of component λ at time t and the average $\langle \rangle_{\text{is}}$ is over a (possibly non-equilibrium) initial state (is), which has to be specified for the particular problem that one wants to study. The Green's function $G_\lambda(\mathbf{r}, \mathbf{r}', t)$ can be interpreted as the probability that particle i of component λ was displaced over \mathbf{r} in a time t given that it started at \mathbf{r}' . Note that the Green's functions do not depend on i because particles of the same kind are indistinguishable.

Although the Green's function approach is aimed primarily at non-equilibrium systems, we will restrict ourselves here only to equilibrium systems, because the time scales for the validity of the expansion to be presented below are expected to be similar in equilibrium and not too far from equilibrium systems, and the equilibrium system is much easier to deal with from a numerical point of view. In the equilibrium case, the Green's functions become independent of \mathbf{r}' because the system is homogeneous and are then identical to the Van Hove self-correlation functions $G_s^\lambda(\mathbf{r}, t)$ (with λ a component) defined as [22]

$$G_s^\lambda(\mathbf{r}, t) = \frac{1}{N_\lambda} \sum_{i=1}^{N_\lambda} \langle \delta[\mathbf{r} + \mathbf{r}_{\lambda i}(0) - \mathbf{r}_{\lambda i}(t)] \rangle, \quad (10)$$

where the subscript s refers to G_s^λ being a self-correlation function of a single particle. The average $\langle \rangle$ is here taken over the canonical equilibrium ensemble ρ_{eq} given in (4). To see

that (10) is the equilibrium variant of (9), note that each term on the right-hand side of (10) gives the same contribution to the sum due to the indistinguishability of particles of the same component. Thus one can also write

$$G_s^\lambda(\mathbf{r}, t) = \langle \delta[\mathbf{r} + \mathbf{r}_{\lambda 1}(0) - \mathbf{r}_{\lambda 1}(t)] \rangle, \quad (11)$$

where particle 1 of component λ is used as a representative particle of that component. The expression for the Van Hove self-correlation function in (11) coincides with that for the Green's function in (9) in cases where the Green's functions have no \mathbf{r}' dependence, i.e. in equilibrium. Note that like the Green's function, the Van Hove self-correlation function $G_s^\lambda(\mathbf{r}, t)$ can therefore be interpreted as the probability that a single fluid particle of component λ has experienced a displacement \mathbf{r} in a time t .

The Fourier transform of the Van Hove self-correlation function is the self-scattering function $F_s^\lambda(\mathbf{k}, t)$ [22], which is given by

$$F_s^\lambda(k, t) = \langle e^{i\mathbf{k} \cdot [\mathbf{r}_{\lambda 1}(t) - \mathbf{r}_{\lambda 1}(0)]} \rangle = \langle e^{ik\Delta x_{\lambda 1}(t)} \rangle. \quad (12)$$

Here $\mathbf{k} = k\hat{\mathbf{k}}$ is a wavevector with length k along the unit vector $\hat{\mathbf{k}}$ and

$$\Delta x_{\lambda 1}(t) = \hat{\mathbf{k}} \cdot [\mathbf{r}_{\lambda 1}(t) - \mathbf{r}_{\lambda 1}(0)] \quad (13)$$

denotes the displacement of particle 1 of component λ along the direction $\hat{\mathbf{k}}$ at a time t . The self-scattering functions can be measured by incoherent neutron scattering experiments [23].

According to elementary probability theory [24] one can interpret $\log F_s^\lambda(k, t)$ as the cumulant generating function of $\Delta x_{\lambda 1}(t)$, where $\Delta x_{\lambda 1}(t)$ is considered to be a random variable, so that $F_s^\lambda(k, t)$ can be written in the following form:

$$F_s^\lambda(k, t) = \exp \left[\sum_{n=1}^{\infty} \frac{\kappa_n^\lambda}{n!} (ik)^n \right]. \quad (14)$$

Here κ_n^λ is called the n th cumulant of the displacement $\Delta x_{\lambda 1}(t)$. The behaviour of these cumulants as a function of time has been investigated in the context of incoherent neutron scattering by Schofield [25] and Sears [26]. They showed that for equilibrium systems, the cumulants (κ_n for $n = 2, 4, 6$) have the following behaviour at small times: $\kappa_2 \sim O(t^2)$, $\kappa_4 \sim O(t^8)$ and $\kappa_6 \sim O(t^{12})$, while the odd cumulants vanish in equilibrium. This behaviour suggested a generalization, which has recently been obtained for a certain class of physical systems as a theorem [18]. For a class of classical systems which includes systems with smooth potentials⁴ in canonical equilibrium, it was shown that the $\kappa_n^\lambda(t)$ have the following form:

$$\kappa_n^\lambda = \begin{cases} c_n^\lambda t^n + O(t^{n+1}) & \text{for } n < 3, \\ c_n^\lambda t^{2n} + O(t^{2n+1}) & \text{for } n \geq 3. \end{cases} \quad (15)$$

where c_n^λ are coefficients independent of t . We see from (14) that for sufficiently small wavevectors k , $F_s^\lambda(k, t) \approx \exp[-\kappa_2^\lambda k^2/2]$. Since $F_s^\lambda(k, t)$ is then approximately Gaussian in k , we would expect that its inverse Fourier transform, the Van Hove self-correlation function $G_s^\lambda(\mathbf{r}, t)$, is also approximately Gaussian in \mathbf{r} . The corrections to the Gaussian behaviour of $F_s^\lambda(k, t)$ are given by the terms in the series in (14) with $n > 2$. Taking the inverse Fourier transform of (14), one can show that the Van Hove self-correlation function is of the form of a Gaussian plus corrections [18]:

$$G_s^\lambda(\mathbf{r}, t) = \frac{\exp(-w^2)}{\sqrt{2\pi\kappa_2^\lambda}} \left[1 + \frac{\kappa_4^\lambda H_4(w)}{4!4[\kappa_2^\lambda]^2} + \frac{\kappa_6^\lambda H_6(w)}{6!8[\kappa_2^\lambda]^3} + \dots \right]. \quad (16)$$

⁴ The LJ potential is not truly smooth because it diverges at $r = 0$. However, in equilibrium, this point has a vanishingly small probability, so that the LJ potential may be treated as effectively smooth.

Here H_n is the n th Hermite polynomial and $w = r/\sqrt{2\kappa_2^\lambda}$ a dimensionless length. Substituting (15) in (16), the Van Hove self-correlation function can be expressed as a time series of the form

$$G_s^\lambda(r, t) = \frac{\exp(-w^2)}{\sqrt{2\pi\kappa_2^\lambda}} \left[1 + \frac{c_4^\lambda m_\lambda^2 t^4}{96T^2} H_4(w) + \frac{c_6^\lambda m_\lambda^3 t^6}{5760T^3} H_6(w) + \dots \right], \quad (17)$$

where we used that in equilibrium $c_2^\lambda = \langle v_{\lambda 1}^2 \rangle = T/m_\lambda$.

There are a few systems for which all the c_n^λ for $n > 2$ are zero, leading to Gaussian Van Hove self-correlation functions. These systems are the ideal gas and systems with only harmonic forces, whose equations of motion are linear. For nonlinear systems, however, the right-hand side of (17) is a series in increasing even powers of t . It is natural to expect that for a small enough t , the successive terms in these series should rapidly decrease. This would mean that the series converges and that one could use a finite number of terms, or even just the Gaussian, as a good approximation to the whole series. Applying the general rule that a series $\sum_{n=0}^{\infty} a_n$ converges if $\lim_{n \rightarrow \infty} |a_{n+1}/a_n| < 1$ to the series in (17), where $a_n \propto c_{2n}^\lambda t^{2n}$, it follows that the time scale below which the decrease in the terms occurs depends critically on the coefficients c_{2n}^λ or in particular on ratios of successive c_{2n}^λ as n approaches infinity. Infinitely large values of n are, of course, beyond the reach of numerical computation, but to get an estimate for the time scales, we numerically evaluated c_{2n}^λ s for the LJ liquid for finite n up to $n = 3$ and the corresponding time scales for the decrease in the terms of the series.

4. Time scales

As explained above, to numerically estimate the time scales up to which the series expansion of the Van Hove self-correlation functions G_s^λ (with $\lambda = A$ or B) in (17) may converge or at least be useful, we are interested in the first few terms of the series. The terms in (17) which are of importance are then the coefficients c_4^λ and c_6^λ . Expressions for these coefficients are derived in section 5, while in section 6 the results of their numerical evaluation in simulations are presented.

For sufficiently small times t , every successive term in the series in (17) would approach zero more rapidly than the previous term because of a larger power of t associated with it. This gives us a simple relation to check when we could expect the terms in the series to decrease. The first estimate of a time scale, to be denoted by τ_G^λ , follows from the criterion that for $t = \tau_G^\lambda$, the first term in the brackets in (17), i.e. 1, is of the same order of magnitude as the next term, i.e. $c_4^\lambda m_\lambda^2 t^4 H_4(w)/(96T^2)$. To find the order of magnitude of the latter, we need an order of magnitude estimate for $H_4(w)$, which we find as follows. The prefactor e^{-w^2} in (17) suggests that $w = O(1)$, since otherwise G_s^λ would be extremely small. The Hermite polynomial $H_4(w)$ contains no physical parameters, only numerical factors which are also of $O(1)$, so we conclude that $H_4(w) = O(1)$. The second term in (17) is therefore of the order of the first term at $t = \tau_G$ with $c_4^\lambda m_\lambda^2 [\tau_G^\lambda]^4 / (96T^2) = O(1)$, yielding

$$\tau_G^\lambda = \left(\frac{96}{|c_4^\lambda|} \right)^{1/4} \sqrt{\frac{T}{m_\lambda}}. \quad (18)$$

This τ_G^λ expresses on what time scale a Gaussian approximation to G_s^λ will break down, while for time scales somewhat less than τ_G^λ , the Gaussian distribution could be supposed to be a good approximation.

The next simplest estimate of a time scale, to be denoted by τ_*^λ , is determined by the time $t = \tau_*^\lambda$ when the second and third terms in the square brackets in (17) become comparable, i.e. when

$$\left| \frac{c_4^\lambda m_\lambda^2 t^4}{96T^2} H_4(w) \right| = \left| \frac{c_6^\lambda m_\lambda^3 t^6}{5760T^3} H_6(w) \right|, \quad (19)$$

which, using the same argument as (18) to show that typical values of $H_4(w)$ and $H_6(w)$ are $O(1)$, leads to

$$\tau_*^\lambda = \left(\frac{60|c_4^\lambda|}{|c_6^\lambda|} \right)^{1/2} \sqrt{\frac{T}{m_\lambda}}. \quad (20)$$

This τ_*^λ also defines a time scale below which the subsequent terms in the series in (17) should decrease in magnitude. Thus, for time scales sufficiently less than τ_*^λ , the c_6^λ term can be neglected compared with the c_4^λ term in (17), but for time scales larger than τ_*^λ , the c_6^λ term certainly needs to be taken into account.

One could in principle get additional time scale estimates τ_n^λ by including higher order terms in (17) and comparing the n th with the $n+1$ st term. Note that then τ_G^λ is equal to τ_1^λ and τ_*^λ is equal to τ_2^λ , respectively. If the limit $\tau^\lambda = \lim_{n \rightarrow \infty} \tau_n^\lambda$ exists, the series in (17) converges for all $t < \tau^\lambda$. In simulations, we cannot take this limit, but we will see that τ_G^λ and τ_*^λ have similar orders of magnitude, suggesting that τ_G^λ and τ_*^λ might be reasonable estimates of the actual time scale of convergence of (17).

5. Expressions for the coefficients c_4^λ and c_6^λ

5.1. General expressions

We first discuss the analytical expressions for the coefficients c_n^λ in terms of the so-called multivariate cumulants based on [18]. The general relation between moments and cumulants is given in the appendix. For short times, the $\kappa_n^\lambda(t)$ have the form given by (15), where for $n \geq 3$ the scaling coefficients c_n^λ s are given by [18]

$$c_n^\lambda = \underbrace{\sum_{n_1=0}^n \cdots \sum_{n_{n+1}=0}^n}_{\substack{\sum_{\gamma=1}^{n+1} n_\gamma = n \\ \sum_{\gamma=1}^{n+1} \gamma n_\gamma = 2n}} \frac{n!}{\prod_{\gamma=1}^{n+1} [n_\gamma! (\gamma!)^{n_\gamma}]} \langle \langle Y_{\lambda 1}^{[n_1]}, \dots, Y_{\lambda n+1}^{[n_{n+1}]} \rangle \rangle. \quad (21)$$

Here, $\langle \langle Y_{\lambda 1}^{[n_1]}, \dots, Y_{\lambda n+1}^{[n_{n+1}]} \rangle \rangle$ is a notation introduced in [18] for a multivariate cumulant, which is a multivariate moment with all possible factorizations subtracted. In this notation, quantities separated by semicolons are treated as separate random variables and if a quantity has a superscript within square brackets, it denotes the number of repetitions of that particular quantity, e.g. $\langle \langle Y_{\lambda 1}^{[3]} \rangle \rangle \equiv \langle \langle Y_{\lambda 1}; Y_{\lambda 1}; Y_{\lambda 1} \rangle \rangle$ (see appendix). Furthermore, $Y_{\lambda \gamma}$ is defined as

$$Y_{\lambda \gamma} = \left. \frac{d^\gamma \Delta x_{\lambda 1}(t)}{dt^\gamma} \right|_{t=0}, \quad (22)$$

with $\Delta x_{\lambda 1}(t)$ defined in (13). Note that we deviate here from the notation in [18], where the cumulants were expressed in terms of $X_{\lambda \gamma} = Y_{\lambda \gamma} / \gamma!$ instead of in terms of $Y_{\lambda \gamma}$.

By writing out the sums in (21) for $n = 4$ and $n = 6$, one finds the following expressions for c_4^λ and c_6^λ :

$$c_4^\lambda = \frac{1}{30} \langle \langle Y_{\lambda 1}^{[3]}, Y_{\lambda 5} \rangle \rangle + \frac{1}{6} \langle \langle Y_{\lambda 1}^{[2]}, Y_{\lambda 3}^{[2]} \rangle \rangle + \frac{1}{4} \langle \langle Y_{\lambda 1}^{[2]}, Y_{\lambda 2}; Y_{\lambda 4} \rangle \rangle \\ + \frac{1}{2} \langle \langle Y_{\lambda 1}; Y_{\lambda 2}^{[2]}, Y_{\lambda 3} \rangle \rangle + \frac{1}{16} \langle \langle Y_{\lambda 2}^{[4]} \rangle \rangle, \quad (23)$$

$$c_6^\lambda = \frac{1}{840} \langle \langle Y_{\lambda 1}^{[5]}, Y_{\lambda 7} \rangle \rangle + \frac{1}{48} \langle \langle Y_{\lambda 1}^{[4]}, Y_{\lambda 2}; Y_{\lambda 6} \rangle \rangle + \frac{1}{24} \langle \langle Y_{\lambda 1}^{[4]}, Y_{\lambda 3}; Y_{\lambda 5} \rangle \rangle + \frac{5}{192} \langle \langle Y_{\lambda 1}^{[4]}, Y_{\lambda 4}^{[2]} \rangle \rangle \\ + \frac{1}{8} \langle \langle Y_{\lambda 1}^{[3]}, Y_{\lambda 2}^{[2]}, Y_{\lambda 5} \rangle \rangle + \frac{5}{54} \langle \langle Y_{\lambda 1}^{[3]}, Y_{\lambda 3}^{[3]} \rangle \rangle + \frac{5}{16} \langle \langle Y_{\lambda 1}^{[2]}, Y_{\lambda 2}^{[3]}, Y_{\lambda 4} \rangle \rangle + \frac{1}{64} \langle \langle Y_{\lambda 2}^{[6]} \rangle \rangle \\ + \frac{5}{4} \langle \langle Y_{\lambda 1}^{[2]}, Y_{\lambda 2}^{[2]}, Y_{\lambda 3}^{[2]} \rangle \rangle + \frac{5}{16} \langle \langle Y_{\lambda 1}; Y_{\lambda 2}^{[4]}, Y_{\lambda 3} \rangle \rangle + \frac{5}{12} \langle \langle Y_{\lambda 1}^{[3]}, Y_{\lambda 2}; Y_{\lambda 3}; Y_{\lambda 4} \rangle \rangle. \quad (24)$$

To evaluate these expressions, we need the explicit expressions for the $Y_{\lambda\gamma}$. Since the $Y_{\lambda\gamma}$ are simply the γ th derivative of $\Delta x_{\lambda 1}$, they can be found by straightforward differentiation (cf (7) and (13)). The resulting expressions are polynomials in the velocities of the particles [18]. Below, it will turn out that only the highest power of the velocities in the expression of each $Y_{\lambda\gamma}$ leads to a non-zero contribution to c_4^λ and c_6^λ . It suffices therefore to write only the highest powers in the velocities for the $Y_{\lambda\gamma}$, i.e.

$$Y_{\lambda 1} = v_{\lambda 1x}, \quad (25)$$

$$Y_{\lambda 2} = -\frac{1}{m_\lambda} \frac{\partial U}{\partial x_{\lambda 1}}, \quad (26)$$

$$Y_{\lambda 3} = -\frac{1}{m_\lambda} \sum_{\mu, j} \frac{\partial^2 U}{\partial x_{\lambda 1} \partial \mathbf{r}_{\mu j}} \cdot \mathbf{v}_{\mu j}, \quad (27)$$

$$Y_{\lambda 4} = -\frac{1}{m_\lambda} \sum_{\mu, j} \sum_{v, k} \frac{\partial^3 U}{\partial x_{\lambda 1} \partial \mathbf{r}_{\mu j} \mathbf{r}_{vk}} : \mathbf{v}_{\mu j} \mathbf{v}_{vk} + \mathcal{O}(v^0), \quad (28)$$

$$Y_{\lambda 5} = -\frac{1}{m_\lambda} \sum_{\mu, j} \sum_{v, k} \sum_{\kappa, \ell} \frac{\partial^4 U}{\partial x_{\lambda 1} \partial \mathbf{r}_{\mu j} \mathbf{r}_{vk} \mathbf{r}_{\kappa \ell}} : \mathbf{v}_{\mu j} \mathbf{v}_{vk} \mathbf{v}_{\kappa \ell} + \mathcal{O}(v^1), \quad (29)$$

$$Y_{\lambda 6} = -\frac{1}{m_\lambda} \sum_{\mu, j} \sum_{v, k} \sum_{\kappa, \ell} \sum_{\rho n} \frac{\partial^5 U}{\partial x_{\lambda 1} \partial \mathbf{r}_{\mu j} \mathbf{r}_{vk} \mathbf{r}_{\kappa \ell} \mathbf{r}_{\rho n}} : \mathbf{v}_{\mu j} \mathbf{v}_{vk} \mathbf{v}_{\kappa \ell} \mathbf{v}_{\rho n} + \mathcal{O}(v^2), \quad (30)$$

$$Y_{\lambda 7} = -\frac{1}{m_\lambda} \sum_{\mu, j} \sum_{v, k} \sum_{\kappa, \ell} \sum_{\rho n} \sum_{\tau p} \frac{\partial^6 U}{\partial x_{\lambda 1} \partial \mathbf{r}_{\mu j} \mathbf{r}_{vk} \mathbf{r}_{\kappa \ell} \mathbf{r}_{\rho n} \mathbf{r}_{\tau p}} : \mathbf{v}_{\mu j} \mathbf{v}_{vk} \mathbf{v}_{\kappa \ell} \mathbf{v}_{\rho n} \mathbf{v}_{\tau p} + \mathcal{O}(v^3), \quad (31)$$

where each sum over two indices denotes a sum over the components A and B for the Greek index and a sum over the particles of that component for the Latin index, while $\mathcal{O}(v^n)$ represents terms which are a polynomial of order n in the velocities.

5.2. Simplifications for equilibrium systems

In equilibrium, the velocities are independent Gaussian distributed variables with zero mean (cf (4) and (5)), which allows some simplifications in the expressions for c_4^λ and c_6^λ in (23) and (24), respectively. These simplifications will not only lead to shorter expressions but will also reduce the number of quantities inside each cumulant, i.e. it will reduce the order of the cumulants. This is numerically advantageous since higher order cumulants tend to require more statistics to keep the error small.

The first simplification is that, given the Gaussian nature of the velocities, theorem A of [18] can be applied to show that the terms denoted by $\mathcal{O}(v^n)$ in (28)–(31) do not contribute to the right-hand side of (23) and (24), because they contribute cumulants which contain fewer powers of the velocity than the number of velocity factors $Y_{\lambda 1} = v_{x\lambda 1}$ in the cumulants, and according to theorem A, such cumulants are zero (see the appendix in [18] for details). On the other hand, the first terms on the right-hand sides of (28)–(31) contain just enough powers of the velocities to match the number of factors of $Y_{\lambda 1} = v_{x\lambda 1}$ in the cumulants in (23) and (24) so that theorem A does not apply and they might yield a non-zero result. Thus only these terms in (28)–(31) need to be taken into account.

The next simplification involves the average over the velocities, which can be taken separately from the average over the positions because of the factored form of the canonical equilibrium distribution given in (4). Thus, canonical averages can be taken in two steps: first an average over velocities and then an average over positions. To apply this two-step process to cumulants, one needs to relate the cumulants to averages. Using (A.3), the cumulants on the right-hand sides of (23) and (24) can be written in terms of moments which are simply averages of products of factors of $Y_{\lambda\gamma}$. For velocity averages of products of independent Gaussian distributed velocities with zero mean, we can use Wick's theorem which states that the average can be obtained by pairing the velocities in all possible ways and then taking the average for each pair separately. Note that the average of two velocities $v_{\mu_1 i_1}$ and $v_{\mu_2 i_2}$ is

$$\langle v_{\mu_1 i_1} v_{\mu_2 i_2} \rangle_v = \frac{T}{m_{\mu_1}} \delta_{\mu_1 \mu_2} \delta_{i_1 i_2}, \quad (32)$$

where the subscript v of the brackets indicates that only the average over velocities is performed. Afterwards, the average over positions, denoted by $\langle \rangle_r$, still needs to be performed to obtain the full average.

The straightforward method of writing the cumulants out in terms of moments introduces a lot of subtraction terms, which can be largely avoided by formulating a similar Wick's rule for cumulants. However, the two-step nature of the averaging process, involving velocity as well as position averages, is a complicating factor here. Forgetting for the moment about the position average, for Gaussian distributed velocities, cumulants can be computed similarly as averages, i.e. using (32), with the distinction that there be only 'connected contributions', in the sense that the pairing of velocities be such that all expressions in the cumulant are connected to each other. To give an example, for the cumulant $\langle \langle v_i v_j; v_k v_l \rangle \rangle_v$, the term $\langle v_i v_j \rangle_v \langle v_k v_l \rangle_v$ does not connect the expressions $v_i v_j$ and $v_k v_l$, and therefore does not contribute, while the terms $\langle v_i v_k \rangle_v \langle v_j v_l \rangle_v$ and $\langle v_i v_l \rangle_v \langle v_j v_k \rangle_v$ do connect the two, so that $\langle \langle v_i v_j; v_k v_l \rangle \rangle_v = \langle v_i v_k \rangle_v \langle v_j v_l \rangle_v + \langle v_i v_l \rangle_v \langle v_j v_k \rangle_v$. However, when averaging with ρ_{eq} in (4), there is a second, non-Gaussian, average, namely, over the positions. As a consequence, although a term like $\langle \frac{\partial^2 U}{\partial r_i \partial r_j} v_i v_j \rangle_v \langle \frac{\partial^2 U}{\partial r_k \partial r_l} v_k v_l \rangle_v$ may seem disconnected and therefore not to contribute to the cumulant $\langle \langle \frac{\partial^2 U}{\partial r_i \partial r_j} v_i v_j; \frac{\partial^2 U}{\partial r_k \partial r_l} v_k v_l \rangle \rangle$, the second average over positions will, as it were, reconnect the parts. One can show that such seemingly disconnected expressions (as far as the velocities are concerned) still yield a contribution to the cumulant which is equal to the position cumulant of the factors, i.e. $\langle \langle \langle \frac{\partial^2 U}{\partial r_i \partial r_j} v_i v_j \rangle; \langle \frac{\partial^2 U}{\partial r_k \partial r_l} v_k v_l \rangle \rangle_r = \langle \langle \frac{\partial^2 U}{\partial r_i \partial r_j}; \frac{\partial^2 U}{\partial r_k \partial r_l} \rangle \rangle_r \langle v_i v_j \rangle_v \langle v_k v_l \rangle_v$, where the subscript r denotes a cumulant over the positions only.

With these rules on how to compute cumulants, we now return to the expressions for c_4^λ and c_6^λ in (23) and (24), respectively. One easily checks that to get connected contributions, all the factors $Y_{\lambda 1} = v_{x\lambda 1}$ in the cumulants in (23) and (24) must be paired with velocities in the other $Y_{\lambda\gamma}$. If n_1 is the number of factors of $Y_{\lambda 1}$ in a cumulant, this introduces a factor $n_1!$ due to the number of ways one can pair two sets of n_1 velocities. Furthermore, because of Kronecker

delta's in (32), all summations from (27)–(31) can easily be performed, and one finds

$$c_4^\lambda = \frac{1}{m_\lambda^4} \left[-\frac{T^3}{5} \left\langle \left\langle \frac{\partial^4 U}{\partial x_{\lambda 1}^4} \right\rangle \right\rangle_r + \frac{T^2}{3} \left\langle \left\langle \left(\frac{\partial^2 U}{\partial x_{\lambda 1}^2} \right)^{[2]} \right\rangle \right\rangle_r + \frac{T^2}{2} \left\langle \left\langle \frac{\partial U}{\partial x_{\lambda 1}}; \frac{\partial^3 U}{\partial x_{\lambda 1}^3} \right\rangle \right\rangle_r - \frac{T}{2} \left\langle \left\langle \left(\frac{\partial U}{\partial x_{\lambda 1}} \right)^{[2]}; \frac{\partial^2 U}{\partial x_{\lambda 1}^2} \right\rangle \right\rangle_r + \frac{1}{16} \left\langle \left\langle \left(\frac{\partial U}{\partial x_{\lambda 1}} \right)^{[4]} \right\rangle \right\rangle_r \right], \quad (33)$$

$$c_6^\lambda = \frac{1}{m_\lambda^6} \left[-\frac{T^5}{7} \left\langle \left\langle \frac{\partial^6 U}{\partial x_{\lambda 1}^6} \right\rangle \right\rangle_r + \frac{T^4}{2} \left\langle \left\langle \frac{\partial U}{\partial x_{\lambda 1}}; \frac{\partial^5 U}{\partial x_{\lambda 1}^5} \right\rangle \right\rangle_r + T^4 \left\langle \left\langle \frac{\partial^2 U}{\partial x_{\lambda 1}^2}; \frac{\partial^4 U}{\partial x_{\lambda 1}^4} \right\rangle \right\rangle_r + \frac{5T^4}{8} \left\langle \left\langle \left(\frac{\partial^3 U}{\partial x_{\lambda 1}^3} \right)^{[2]} \right\rangle \right\rangle_r - \frac{3T^3}{4} \left\langle \left\langle \left(\frac{\partial U}{\partial x_{\lambda 1}} \right)^{[2]}; \frac{\partial^4 U}{\partial x_{\lambda 1}^4} \right\rangle \right\rangle_r - \frac{5T^3}{9} \left\langle \left\langle \left(\frac{\partial^2 U}{\partial x_{\lambda 1}^2} \right)^{[3]} \right\rangle \right\rangle_r + \frac{5T^2}{8} \left\langle \left\langle \left(\frac{\partial U}{\partial x_{\lambda 1}} \right)^{[3]}; \frac{\partial^3 U}{\partial x_{\lambda 1}^3} \right\rangle \right\rangle_r - \frac{1}{64} \left\langle \left\langle \left(\frac{\partial U}{\partial x_{\lambda 1}} \right)^{[6]} \right\rangle \right\rangle_r + \frac{5T^2}{2} \left\langle \left\langle \left(\frac{\partial U}{\partial x_{\lambda 1}} \right)^{[2]}; \left(\frac{\partial^2 U}{\partial x_{\lambda 1}^2} \right)^{[2]} \right\rangle \right\rangle_r - \frac{5T}{16} \left\langle \left\langle \left(\frac{\partial U}{\partial x_{\lambda 1}} \right)^{[4]}; \frac{\partial^2 U}{\partial x_{\lambda 1}^2} \right\rangle \right\rangle_r - \frac{5T^3}{2} \left\langle \left\langle \frac{\partial U}{\partial x_{\lambda 1}}; \frac{\partial^2 U}{\partial x_{\lambda 1}^2}; \frac{\partial^3 U}{\partial x_{\lambda 1}^3} \right\rangle \right\rangle_r \right]. \quad (34)$$

Here the same notation has been used as explained in (21) and in the appendix.

The above expressions can still be further simplified for systems in canonical equilibrium, using the following identity due to Yvon [28, 29]:

$$\left\langle \frac{\partial U}{\partial x_{\lambda 1}} B \right\rangle_r = T \left\langle \frac{\partial B}{\partial x_{\lambda 1}} \right\rangle_r, \quad (35)$$

for any function B of the position of the particles, as can be proved by partial integration. While we will not present the lengthy details here, this identity can be used to find linear relations between the expressions on the right-hand sides of (36) and (37), which allow us to rewrite the expressions for c_4^λ and c_6^λ in a variety of ways. Among those, we choose

$$c_4^\lambda = \frac{1}{m_\lambda^4} \left[-\frac{T^3}{80} \left\langle \left\langle \frac{\partial^4 U}{\partial x_{\lambda 1}^4} \right\rangle \right\rangle_r + \frac{T^2}{48} \left\langle \left\langle \left(\frac{\partial^2 U}{\partial x_{\lambda 1}^2} \right)^{[2]} \right\rangle \right\rangle_r \right], \quad (36)$$

$$c_6^\lambda = \frac{1}{m_\lambda^6} \left[-\frac{T^5}{448} \left\langle \left\langle \frac{\partial^6 U}{\partial x_{\lambda 1}^6} \right\rangle \right\rangle_r + \frac{T^4}{64} \left\langle \left\langle \frac{\partial^2 U}{\partial x_{\lambda 1}^2}; \frac{\partial^4 U}{\partial x_{\lambda 1}^4} \right\rangle \right\rangle_r - \frac{5T^3}{576} \left\langle \left\langle \left(\frac{\partial^2 U}{\partial x_{\lambda 1}^2} \right)^{[3]} \right\rangle \right\rangle_r \right]. \quad (37)$$

These equations require at most second and third order cumulants, respectively, which is advantageous since numerically higher order cumulants tend to produce larger statistical error. They agree with the expressions found by Sears for a one-component fluid [26]. Note that in the special case of a harmonic potential, derivatives higher than the second vanish, so that then for c_4^λ and c_6^λ only the last terms in (36) and (37), respectively, remain, which only involve the cumulants of the second derivative of the potential. Since the second derivative is constant for a harmonic potential, these cumulants are zero as well, so that the coefficients c_4^λ and c_6^λ are zero, as expected for a linear system.

With this background, next we present the results of the numerical evaluation of the coefficients c_4^λ and c_6^λ for a number of equilibrium systems by means of molecular dynamics simulations, in order to estimate the time scales τ_G^λ and τ_*^λ , which indicate where one could suppose that the first term alone (i.e. the leading Gaussian) or the first few terms (i.e. the Gaussian plus corrections) of the series in (17) can be used as a good approximation to the full Van Hove self-correlation function.

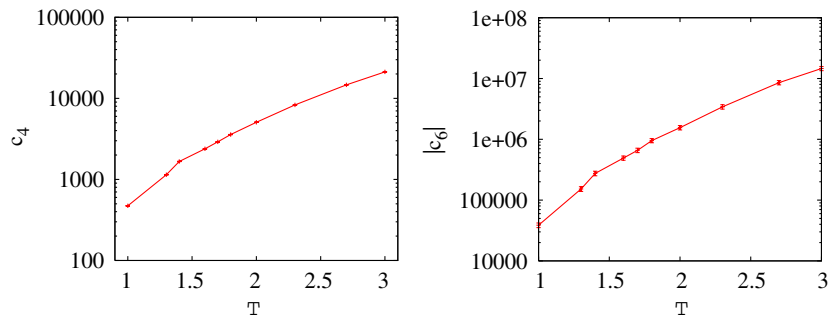


Figure 1. The coefficients c_4 (on the left) and c_6 (on the right) as a function of temperature T for an equilibrium single component LJ fluid with density $\rho = 0.8$. These results are from a MD simulation with $N = 100$ particles, with periodic boundary conditions. All quantities are in the LJ units defined in section 2.

6. Simulation results

6.1. Single component LJ fluid

In this section, we present the numerical result for c_4 and c_6 (cf (36) and (37)) and the resulting time scales τ_G and τ_* (cf (18) and (20)) for a single component fluid of $N = N_A$ LJ particles with periodic boundary conditions in a box of linear size $L = 5$ (in LJ units). Note that we have omitted the component superscript λ here because there is only one component. The results were obtained from molecular dynamics (MD) simulations, for which the initial conditions were drawn from the canonical distribution by employing an isokinetic Gaussian thermostat [27] during the equilibration stage, while the runs themselves were done at constant volume and energy. In the simulation, a potential cutoff of $r_c = 2.5\sigma$ was used and the equations of motion were integrated using the Verlet algorithm [19] with a time step of 2 femtoseconds.

Since τ_G and τ_* will depend on temperature and density, it is of interest to study the dependence of c_4 and c_6 as a function of these two parameters. We studied the temperature dependence by keeping N and ρ fixed at 100 and 0.8, respectively, while temperature values ranging from 1 to 3 were used. For each of these parameter values, data were accumulated once equilibrium had been attained in the simulation and collected every 2 ps in a 8 ps long run, yielding five points per run. This was repeated for 2000 different initial conditions (yielding 10 000 points per temperature) for each temperature value and the results for c_4 and c_6 were averaged over these 2000 runs. To decrease the statistical errors even further, we averaged over all particles of the same kind (i.e. replacing index 1 in (36) and (37) by any index i and averaging the results) as well as over the three directions of space (i.e. replacing x by y and z in (36) and (37) and averaging).

The resulting behaviour of c_4 and c_6 as a function of temperature is shown in figure 1. The data for c_4 in the left panel of figure 1 are consistent with the preliminary data that were presented in [17]. Note that in figure 1, the absolute value of the coefficient c_6 has been plotted. The reason is that the values of c_6 that are found in the simulations are always negative. In figure 2, we plotted the resulting time scales τ_G and τ_* (cf (18) and (20)) as a function of temperature. We see that by increasing the temperature, we moderately decrease these time scales from roughly 2 ps to 1 ps, which are the estimates for the time scales up to which the series in (17) could be supposed to give an accurate approximation to G_s^λ .

The density dependence of c_4 and c_6 was also investigated using the same setup, but keeping the temperature fixed at $T = 1.0$, while the density ranged from $\rho = 0.5$ to $\rho = 1.0$.

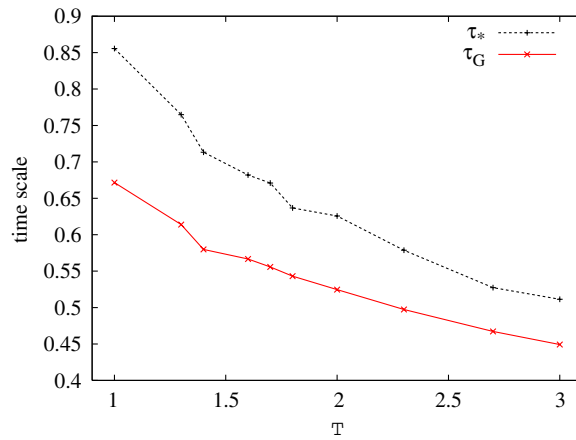


Figure 2. The critical time scales τ_G and τ_* at which the series in (17) for the Van Hove self-correlation function of an equilibrium single component fluid could be supposed to be practicable (cf section 4, below (18) and (20)) as a function of temperature T for a density $\rho = 0.8$. Note that the physical time scales in picoseconds can be calculated by multiplying both τ_* and τ_G by the LJ unit time $\tau_{LJ} = 2.16$ ps.

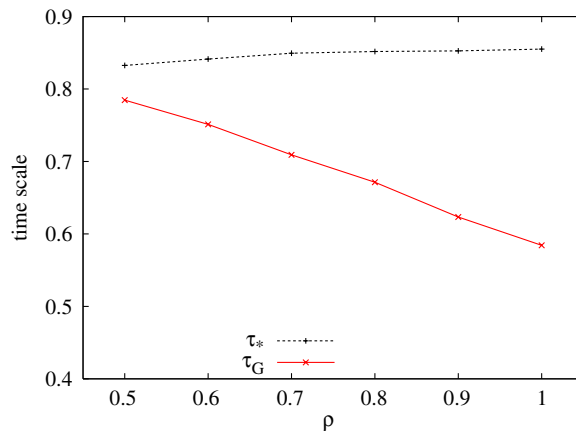


Figure 3. The critical time scales τ_G and τ_* at which the series in (17) for the equilibrium single component fluid could be supposed to be useful (cf section 4, below (18) and (20)) as a function of the density ρ for fixed temperature $T = 1.0$. Note that the physical time scale in picoseconds can be calculated by multiplying both τ_* and τ_G by the LJ unit time $\tau_{LJ} = 2.16$ ps.

The resulting time scales τ_G and τ_* as a function of density are plotted in figure 3. While both time scales remain on the order of 1 or 2 ps under changes in the density, we see that the two time scales τ_G and τ_* behave quite differently; whereas the time scale τ_G decreases moderately with increasing density, indicating that the first correction term in (17) becomes important somewhat sooner for higher than for lower densities, the time scale τ_* is virtually constant as a function of density and bigger than τ_G , indicating that the second correction term in (17) becomes important at a slightly larger time scale. However, the order of magnitude of these two time scales is so similar (i.e. both of picosecond order) that such a distinction does not appear to be significant.

6.2. Isotopic LJ binary mixture

Our investigation into the cumulants originated in the study of mass transport in binary isotopic mixtures at short time scales [16], and hence we are interested in the time scales τ_G^λ and τ_*^λ in binary isotopic mixtures as well. From the expressions for the time scales in (18) and (20) as well as for the coefficients c_4^λ and c_6^λ in (33) and (34), respectively, one can readily deduce that $c_4^\lambda \propto m_\lambda^{-4}$ and $c_6^\lambda \propto m_\lambda^{-6}$. Using this in (18) and (20), one sees that the time scales τ_G^λ and τ_*^λ simply scale as the square root of the mass. The remaining parts of the coefficients only involve the potential, which in an isotopic mixture is the same as for a pure LJ system. Therefore, no new simulations are needed for this case; the time scales are those of the pure LJ system, multiplied by the square root of the mass ratio of the components and the original LJ particles, i.e.

$$\tau_G^\lambda = \tau_G \sqrt{\frac{m_\lambda}{m}}, \quad (38)$$

$$\tau_*^\lambda = \tau_* \sqrt{\frac{m_\lambda}{m}}, \quad (39)$$

where m is the mass of the particles in a single component LJ fluid.

Since in Nature, there are no isotopes with large mass ratios, we conclude that for isotopic binary mixtures the time scales at which the series in (17) can be supposed to be useful are the same as those for a single LJ fluid, i.e. of the order of a picosecond.

6.3. Nanofluids

A nanofluid is a binary mixture of LJ fluid particles (A particles) and nanoparticles (B particles). For such a mixture, the time scales τ_G^A and τ_*^A and τ_G^B and τ_*^B need not be the same. They were investigated here using the same approach as above, but there are additional numerical challenges. First of all, for large B particles, the typical relaxation and correlation times (say of the particle velocity) grow with increasing R due to the increased inertia of the B particle. As a result, it takes longer to equilibrate such a system, and one obtains fewer independent data points per time unit. Secondly, since the B particle is already quite large, to surround it with a liquid-like fluid of A particles requires a large number of A particles. This increase in the number of particles causes a substantial slowdown of the simulations. To keep down the number of A particles, one takes as few B particles as possible. This contributes to a third difficulty, namely, that for the B particles, there are fewer particles to average over, leading to poorer statistics.

Given these difficulties, fewer runs can be performed in a reasonable time for these systems and as a result the error bars on the data for the B particles are substantially larger than those for the A particles and of the LJ fluids of the previous sections. Nonetheless, we have been able to extract estimates for the time scales at which the series in (17) could be supposed to be also useful for these systems.

For the simulations of the nanofluid, two temperature values were taken: a low temperature $T = 1$ (corresponding to 122 K for argon) and a high temperature $T = 3$ (366 K, chosen to be closer to room temperature). The simulated system contained $N_B = 1, 2$ or 3 nanoparticles of size $R = 2, 4$ or 6 (i.e. all nine combinations were studied). The linear box size was $L = 30$ so that the number density of the nanoparticles had the values $\rho_B = 3.7 \times 10^{-5}, 7.4 \times 10^{-5}$ and 1.1×10^{-4} for $N_B = 1, 2$ and 3, respectively. To keep the properties of the LJ fluid in which the nanoparticles are suspended constant, the remainder of the box was filled with LJ particles with a fixed number density $\rho_A = N_A / (L^3 - \frac{4}{3}\pi R^3 N_B)$, which was, somewhat arbitrarily, chosen

Table 1. The coefficients c_4^λ and c_6^λ for the LJ particles (A) and the nanoparticles (B) in the nanofluid of section 6.3 at $T = 1$.

		$R = 2$	$R = 4$	$R = 6$
$N_B = 1$	c_4^A	283.6 ± 0.4	288.4 ± 0.5	296 ± 0.7
	c_6^A	$-24\,524 \pm 477$	$-24\,865 \pm 554$	$-25\,369 \pm 690$
	c_4^B	0.036 ± 0.002	$(29.3 \pm 1.7) \times 10^{-6}$	$(0.40 \pm 0.03) \times 10^{-6}$
	c_6^B	-0.066 ± 0.037	$(-1.2 \pm 0.6) \times 10^{-6}$	$(-1.6 \pm 0.9) \times 10^{-9}$
$N_B = 2$	c_4^A	284.8 ± 0.7	293.5 ± 0.9	308 ± 1
	c_6^A	$-24\,777 \pm 788$	$-25\,100 \pm 751$	$-26\,052 \pm 1209$
	c_4^B	0.036 ± 0.002	$(29 \pm 2) \times 10^{-6}$	$(0.52 \pm 0.05) \times 10^{-6}$
	c_6^B	-0.079 ± 0.058	$(-1.0 \pm 0.6) \times 10^{-6}$	$(-2.0 \pm 1.5) \times 10^{-9}$
$N_B = 3$	c_4^A	289.1 ± 0.9	300 ± 1	314 ± 2
	c_6^A	$-25\,500 \pm 1039$	$-25\,717 \pm 1170$	$-26\,368 \pm 1257$
	c_4^B	0.041 ± 0.002	$(41 \pm 2) \times 10^{-6}$	$(0.78 \pm 0.06) \times 10^{-6}$
	c_6^B	-0.13 ± 0.10	$(-2.2 \pm 1.2) \times 10^{-6}$	$(-3 \pm 2) \times 10^{-9}$

Table 2. The coefficients c_4^λ and c_6^λ for the LJ particles (A) and the nanoparticles (B) in the nanofluid of section 6.3 at $T = 3$.

		$R = 2$	$R = 4$	$R = 6$
$N_B = 1$	c_4^A	9042 ± 7	9034 ± 7	9123 ± 6
	c_6^A	$(-6.4 \pm 0.12) \times 10^6$	$(-6.3 \pm 0.11) \times 10^6$	$(-6.4 \pm 0.11) \times 10^6$
	c_4^B	17 ± 1	$(22 \pm 2) \times 10^{-3}$	$(357 \pm 54) \times 10^{-6}$
	c_6^B	-442 ± 291	$(-11 \pm 17) \times 10^{-3}$	$(-18 \pm 76) \times 10^{-6}$
$N_B = 2$	c_4^A	9049 ± 8	9163 ± 8	9296 ± 8
	c_6^A	$(-6.4 \pm 0.13) \times 10^6$	$(-6.5 \pm 0.14) \times 10^6$	$(-6.6 \pm 0.12) \times 10^6$
	c_4^B	17 ± 1	$(23 \pm 2) \times 10^{-3}$	$(390 \pm 43) \times 10^{-6}$
	c_6^B	-434 ± 192	$(-13 \pm 17) \times 10^{-3}$	$(-18 \pm 62) \times 10^{-6}$
$N_B = 3$	c_4^A	9087 ± 8	9203 ± 6	9455 ± 160
	c_6^A	$(-6.4 \pm 0.12) \times 10^6$	$(-6.5 \pm 0.1) \times 10^6$	$(-6.8 \pm 0.7) \times 10^6$
	c_4^B	17 ± 1	$(22 \pm 1) \times 10^{-3}$	$(468 \pm 110) \times 10^{-6}$
	c_6^B	-425 ± 198	$(-11 \pm 11) \times 10^{-3}$	$(-4.3 \pm 105) \times 10^{-6}$

to be 0.49, i.e. N_A was chosen such that for given L , R and N_B , ρ_A was as close to 0.49 as possible. This required between $N_A = 11\,912$ and $N_A = 13\,227$ fluid LJ particles, depending on R and N_B . Note that even though the number densities of the nanoparticles are small, by assigning a volume $\frac{4}{3}\pi R^3$ to each nanoparticle, one sees that the volume fraction ranges from 0.124% to 10%. This is a realistic range, as experimental volume fractions are of the order of 1% [1]. We did not investigate much higher volume fractions to avoid possible complicating effects such as aggregation of the nanoparticles.

For the systems with 1 nanoparticle, 100 runs were performed for each of the two temperature values $T = 1$ and $T = 3$, where first the system was equilibrated using an isokinetic Gaussian thermostat, and then the system was run for 8 ps during which the quantities appearing in (36) and (37) were measured. For the systems with $N_B = 2$, 50 runs were performed and for those with $N_B = 3$ the number of runs was 34 (for each temperature value). Because of the isokinetic Gaussian thermostat, the average over these runs approximates the average over the canonical distribution in (4).

The resulting values for c_4^λ and c_6^λ are shown in tables 1 and 2 for $T = 1$ and $T = 3$, respectively. From c_4^λ and (18) we find the time scales τ_G^λ , which are listed in tables 3 and 4

Table 3. The time scales τ_G^λ and τ_*^λ (in LJ units) as follow from c_4^λ and c_6^λ according to (18) and (20) for the LJ particles (A) and the nanoparticles (B) in the nanofluid of section 6.3 at $T = 1$, respectively. Note that the physical time scale in picoseconds can be calculated by multiplying τ_* and τ_G by the LJ unit time $\tau_{LJ} = 2.16$ ps.

		$R = 2$	$R = 4$	$R = 6$
$N_B = 1$	τ_G^A	0.763 ± 0.001	0.759 ± 0.001	0.755 ± 0.001
	τ_*^A	0.833 ± 0.008	0.834 ± 0.009	0.837 ± 0.011
	τ_G^B	2.40 ± 0.03	5.28 ± 0.08	8.45 ± 0.16
	τ_*^B	1.9 ± 0.5	4.7 ± 1.2	8 ± 2
$N_B = 2$	τ_G^A	0.762 ± 0.001	0.756 ± 0.001	0.747 ± 0.001
	τ_*^A	0.830 ± 0.013	0.838 ± 0.013	0.842 ± 0.019
	τ_G^B	2.40 ± 0.03	5.29 ± 0.09	7.91 ± 0.19
	τ_*^B	1.9 ± 0.8	5.2 ± 1.6	8 ± 3
$N_B = 3$	τ_G^A	0.759 ± 0.001	0.752 ± 0.001	0.744 ± 0.001
	τ_*^A	0.825 ± 0.017	0.837 ± 0.019	0.84 ± 0.02
	τ_G^B	2.32 ± 0.03	4.85 ± 0.06	7.15 ± 0.14
	τ_*^B	1.5 ± 0.6	4.1 ± 1.1	8 ± 3

Table 4. The time scales τ_G^λ and τ_*^λ (in LJ units) as follow from c_4^λ and c_6^λ according to (18) and (20) for the LJ particles (A) and the nanoparticles (B), respectively, in the nanofluid of section 6.3 at a temperature of $T = 3$. Note that the physical time scale in picoseconds can be calculated by multiplying τ_* and τ_G by the LJ unit time $\tau_{LJ} = 2.16$ ps.

		$R = 2$	$R = 4$	$R = 6$
$N_B = 1$	τ_G^A	0.5560 ± 0.0001	0.5561 ± 0.0001	0.5547 ± 0.0001
	τ_*^A	0.503 ± 0.005	0.508 ± 0.004	0.508 ± 0.004
	τ_G^B	0.89 ± 0.01	1.75 ± 0.04	2.7 ± 0.1
	τ_*^B	0.88 ± 0.29	2.4 ± 1.9	4 ± 8
$N_B = 2$	τ_G^A	0.5559 ± 0.0001	0.5541 ± 0.0001	0.5547 ± 0.0001
	τ_*^A	0.505 ± 0.005	0.504 ± 0.005	0.508 ± 0.004
	τ_G^B	0.89 ± 0.01	1.73 ± 0.03	2.62 ± 0.07
	τ_*^B	0.88 ± 0.20	2.2 ± 1.5	4 ± 7
$N_B = 3$	τ_G^A	0.5553 ± 0.0001	0.5535 ± 0.0001	0.5498 ± 0.0001
	τ_*^A	0.507 ± 0.005	0.504 ± 0.004	0.50 ± 0.25
	τ_G^B	0.89 ± 0.01	1.74 ± 0.02	2.5 ± 0.15
	τ_*^B	0.90 ± 0.21	2.4 ± 1.2	9 ± 114

for $T = 1$ and $T = 3$, respectively. In tables 1 and 2, one notices the large error estimates for c_6^B (whose values are negative as in the pure LJ case), which may seem to make it hard to draw conclusions from those data. However, according to (37) we only need the square root of this number to estimate τ_*^B , leading to a reduction of the relative error by one-half, which explains why the results for τ_*^B given in tables 3 and 4 are still reasonable *order of magnitude* estimates for all cases except for the combination of physical parameters $R = 6$ and $T = 3$.

We see from tables 3 and 4 that for the LJ fluid particles (A) surrounding the nanoparticles, both time scales τ_G^A and τ_*^A (below which the expansion of the Van Hove self-correlation function around a Gaussian as in (17) may be useful) are on the order of 1 or 2 ps. While they decrease moderately with increasing temperatures, these time scales are relatively insensitive to both the radius and the density of the nanoparticles and are in fact close to their values in the absence of nanoparticles (cf figure 2), which were also on the order of 1–2 ps.

In contrast to this, tables 3 and 4 show that the time scales below which the expansion of the Van Hove self-correlation function of the nanoparticles (B) around a Gaussian could be supposed to be practicable are considerably larger than for the fluid particles, and, in fact, increase with the radius of the nanoparticles up to as much as a factor of 5 for $T = 3$ and a factor of 10 for $T = 1$ for the largest nanoparticle size studied. The time scales decrease upon increasing the density of the nanoparticles, but by a lesser amount, so that the overall time scale below which (17) is useful is still on the order of 5 ps for $T = 3$ and on the order of 10 ps for $T = 1$.

7. Conclusions

We have investigated the short time behaviour of the Van Hove self-correlation function. According to (17), for short times, the Hove self-correlation function can be expressed as a Gaussian plus corrections, which are proportional to increasing powers of t . For short times, this can be re-expressed by the series in (17), which is useful provided the contributions of the correction terms are small. From the form of these correction terms in (17), one sees that they are small at time scales smaller than some critical time scale (τ_G). In this paper, this time scale was investigated for a number of LJ and LJ-based systems. We found that a decrease in the magnitude of the terms in the series (17) occurs below and up to the picosecond time scales for LJ fluid particles and up to the 10 ps time scale for nanoparticles.

Two time scales were in fact calculated: one, denoted by τ_G , estimates when the first correction term to the Gaussian distribution will be small and the other, denoted by τ_* , estimates the time at which the second correction term is as big as the first one. The larger these time scales, the better, since this means that the expansion in (17), i.e. the Gaussian plus two correction terms, or perhaps even just the simple Gaussian prefactor, can be used for all time scales below (and possibly up to) τ_G and τ_* . Note that if these time scales are of similar order of magnitude, as they turned out to be, then they could also be viewed as a possible estimate of the radius of convergence of the series in (17).

We first investigated the coefficients for the equilibrium pure LJ fluid as a function of temperature and concluded that both time scales τ_G and τ_* are reduced as a function of increasing temperature from about 2 to 1 ps. As a function of density, our two estimates of the time scales behave differently. While τ_G decreases by moderate amounts with increasing density, τ_* stays roughly the same. In all cases, though, the time scales are of the order of a picosecond or more. One can qualitatively understand the decreasing trend of the ‘Gaussian’ time scale τ_G for increasing densities, by realizing that the forces between the particles perturb the short time ballistic motion away from its Gaussian character. Since the forces are stronger at higher densities, the deviations from Gaussian behaviour will then occur earlier.

In mixtures, there is a Van Hove self-correlation function for each component, and, correspondingly, the time scales depend on the component whose Van Hove self-correlation function is studied, which is represented by a superscript $\lambda = A$ or B on τ_G and τ_* . We deduced for a binary isotopic mixture that the time scales τ_G^λ and τ_*^λ on which (17) could be supposed to be useful simply scale as the square root of the mass m_λ of the component λ . As said before, since in Nature, isotopes do not have very large mass ratios, for isotopic binary mixtures the time scales at which the series in (17) is useful are of the same order of magnitude as for a one-component fluid, i.e. of the order of a picosecond.

Finally, we studied these time scales in a recently proposed model of a nanofluid [21], and found that the time scales are there of the order of 5–10 ps for the nanoparticles (decreasing with temperature and increasing with radius), while for the fluid particles in that model the time scale is still on the order of a picosecond. The difference in time scales could be due to the larger

mass of the nanoparticles, causing the forces to have less influence on their velocities, which therefore remain close to their original (Gaussian) distribution for a longer time than in a LJ fluid. It is then no surprise that the distribution of displacements for nanoparticles can be described by a Gaussian at longer time scales than for the lighter fluid particles.

One may wonder whether the time scales found in this paper are not so short that the classical description on which they were based breaks down. A simple estimate of the time scale at which appreciable quantum effects can be expected is given by $\hbar/k_B T$, where \hbar is Planck's constant divided by 2π . At room temperature, this is equal to about 25 femtoseconds. Note that all time scales found in this paper were at picosecond or at tens of picosecond scales, i.e. well above this quantum time scale.

Although our results for the time scales τ_G^λ and τ_*^λ are only estimates, they are encouraging for the possible application of Green's function approach to small scale nanometre length and picosecond time scales, since the Van Hove self-correlation functions are equilibrium versions of Green's functions [12–16]. Furthermore, it is expected that the time scales for non-equilibrium systems are similar to those of equilibrium systems, which were on the order of picoseconds for fluid particles and on the order of 10 ps for nanoparticles. This suggests that expansions of the form in (17) can be useful for the Green's function approach for transport problems taking place at and below picosecond time scales and at nanometre length scales in equilibrium and near-equilibrium systems.

Acknowledgments

This work was supported by the Office of Basic Energy Sciences of the US Department of Energy under grant number DE-FG-02-88-ER13847 and under grant PHY-501315 of the Mathematical Physics program of the National Science Foundation.

Appendix. Moments and cumulants

In this appendix we will briefly recall the definitions of the moments and cumulants and how they are related. For more details, see [24].

We first remark that multivariate moments and cumulants are simply moments and cumulants of more than one variable. In general, (multivariate) moments can be defined as follows. For a single random variable x with a distribution $f_1(x)$, the n th moment is $\mu_n = \langle x^n \rangle = \int dx x^n f_1(x)$, while for a pair of random variables x_1 and x_2 with a joint distribution $f_2(x_1, x_2)$, the bivariate moments are $\langle x_1^{n_1} x_2^{n_2} \rangle = \int dx_1 \int dx_2 x_1^{n_1} x_2^{n_2} f_2(x_1, x_2)$, and so on for multivariate moments $\langle x_1^{n_1} \cdots x_q^{n_q} \rangle = \int dx_1 \cdots \int dx_q x_1^{n_1} \cdots x_q^{n_q} f_q(x_1, \dots, x_q)$. One defines the order of a multivariate moment as the sum $\sum_{r=1}^q n_r$. For near-Gaussian (multivariate) distributions, the cumulants are a more convenient way to characterize the distribution than the moments, because the cumulants of order higher than two are zero for a pure Gaussian. For a single variable the general expression for the n th cumulant κ_n in terms of moments $\mu_{k \leq n}$ is

$$\kappa_n = -n! \sum_{\substack{\{p_\ell \geq 0\} \\ \sum_{\ell=1}^{\infty} \ell p_\ell = n}} \left(\sum_{\ell=1}^{\infty} p_\ell - 1 \right)! \prod_{\ell=1}^{\infty} \frac{[-\mu_\ell / \ell!]^{p_\ell}}{p_\ell!}. \quad (\text{A.1})$$

In analogy with the notation $\mu_n = \langle x^n \rangle$ for moments of a random variable x , one often uses the notation $\kappa_n = \langle\langle x^n \rangle\rangle$ for its cumulants [24]. Here, the superscript n inside the double brackets

is not a power, as the example $\langle\langle x^2 \rangle\rangle = \langle x^2 \rangle - \langle x \rangle^2$ shows. To avoid confusion, we denote instead the cumulants as $\langle\langle x^{[n]} \rangle\rangle$. Therefore, instead of (A.1) we can write

$$\langle\langle x^{[n]} \rangle\rangle = -n! \sum_{\substack{\{p_\ell \geq 0\} \\ \sum_{\ell=1}^{\infty} \ell p_\ell = n}} \left(\sum_{\ell=1}^{\infty} p_\ell - 1 \right)! \prod_{\ell=1}^{\infty} \frac{[-\langle x^\ell \rangle / \ell!]^{p_\ell}}{p_\ell!}. \quad (\text{A.2})$$

One can interpret the superscript n between square brackets in this expression as the number of ‘repetitions’ of x . Then, as an alternative to (A.2), one can define the cumulants recursively as the average of the product of these repetitions minus the product of lower order cumulants of all possible groupings of the n repetitions. For instance, for the third order cumulant of the displacement one can write $\langle\langle x^{[3]} \rangle\rangle = \langle x^3 \rangle - 3\langle x \rangle \langle\langle x^{[2]} \rangle\rangle - \langle\langle x \rangle\rangle^3$, where the factor 3 arises from the three ways in which one can group three repetitions into a pair and a single repetition. This expression contains the second order cumulant $\langle\langle x^{[2]} \rangle\rangle$, which can be written as $\langle\langle x^{[2]} \rangle\rangle = \langle x^2 \rangle - \langle x \rangle^2$, while finally $\langle\langle x \rangle\rangle = \langle x \rangle$, leading to $\langle\langle x^{[3]} \rangle\rangle = \langle x^3 \rangle - 3\langle x \rangle \langle x^2 \rangle + 2\langle x \rangle^3$. This is a special case of the general formula (A.2).

Similarly to this univariate case, multivariate cumulants can be represented in terms of the averages, in the following way [18]:

$$\begin{aligned} \langle\langle x_1^{[n_1]}, \dots, x_q^{[n_q]} \rangle\rangle \\ = -n_1! \dots n_q! \sum_{\substack{\{p_{\{\ell\}} \geq 0\} \\ \sum_{\{\ell\}} \ell_j p_{\{\ell\}} = n_j}} \left(\sum_{\{\ell\}} p_{\{\ell\}} - 1 \right)! \prod_{\{\ell\}} \frac{1}{p_{\{\ell\}}!} \left(-\frac{\langle x_1^{\ell_1} \dots x_q^{\ell_q} \rangle}{\ell_1! \dots \ell_q!} \right)^{p_{\{\ell\}}}. \end{aligned} \quad (\text{A.3})$$

In this notation for the cumulants, quantities separated by semicolons are treated as separate random variables and, as above, if a quantity has a superscript within square brackets, it denotes the particular number of repetitions of the quantity. Some examples of multivariate cumulants in terms of multivariate moments are

$$\langle\langle x_1 \rangle\rangle = \langle x_1 \rangle, \quad (\text{A.4})$$

$$\langle\langle x_1; x_2 \rangle\rangle = \langle x_1 x_2 \rangle - \langle x_1 \rangle \langle x_2 \rangle, \quad (\text{A.5})$$

$$\langle\langle x_1; x_2; x_3 \rangle\rangle = \langle x_1 x_2 x_3 \rangle - \langle x_1 x_2 \rangle \langle x_3 \rangle - \langle x_1 x_3 \rangle \langle x_2 \rangle - \langle x_1 \rangle \langle x_2 x_3 \rangle + 2\langle x_1 \rangle \langle x_2 \rangle \langle x_3 \rangle. \quad (\text{A.6})$$

In the main text, the moments μ and cumulants κ occur as moments and cumulants of the displacements of a single particle of a specific component λ in a time t and therefore appear with a superscript λ (and an implicit time argument t). Furthermore, multivariate cumulants appear where the x_γ are replaced by $Y_{\lambda\gamma}$ or by derivatives of the potential, i.e. $\partial^\gamma U / \partial x_{\lambda 1}^\gamma$.

References

- [1] Choi S U S, Xu X, Koblinski P and Yu W 2002 *DOE BES 20th Symp. on Energy Engineering Sciences (Argonne, IL, 20–21 May)*
- [2] Hwang H J, Kwon O-K and Kang J W 2004 *Solid State Commun.* **129** 687–90
- [3] Tang W and Advani S G 2006 *J. Chem. Phys.* **125** 174706
- [4] Chen X, Samia A C S, Lou Y and Burda C 2005 *J. Am. Chem. Soc.* **127** 4372–5
- [5] Verberg R, de Schepper I M and Cohen E G D 1997 *Phys. Rev. E* **55** 3143–58
- [6] Ten Wolde P R and Frenkel D 1997 *Science* **277** 1975
- [7] Pellicane G, Costa D and Caccamo C 2004 *J. Phys.: Condens. Matter* **16** S4923
- [8] Barrat J L and Hansen J-P 2003 *Basic Concepts for Simple and Complex Liquids* (Cambridge: Cambridge University Press)

- [9] Roth M W and Balasubramanya M K 2000 *Phys. Rev. B* **62** 17043–54
- [10] Baletto F and Ferrando R 2005 *Rev. Mod. Phys.* **77** 371
- [11] Szwacki N G, Sadrzadeh A and Yakobson B I 2007 *Phys. Rev. Lett.* **98** 166804
- [12] Kincaid J M 1995 *Phys. Rev. Lett.* **74** 2985–8
- [13] Kincaid J M and Cohen E G D 2002 *Mol. Phys.* **100** 3005–10
- [14] Kincaid J M and Cohen E G D 2002 *J. Stat. Phys.* **109** 361–7
- [15] Kincaid J M and Cohen E G D 2002 *Proc. 20th Symp. on Energy and Engineering Sciences* pp 262–9
- [16] van Zon R and Cohen E G D 2005 *Preprint cond-mat/0508268*
- [17] van Zon R, Ashwin S S and Cohen E G D 2007 *C. R. Physique* **8** 633–40
- [18] van Zon R and Cohen E G D 2006 *J. Stat. Phys.* **123** 1–37
- [19] Frenkel D and Smit B 2002 *Understanding Molecular Simulation. From Algorithms to Applications* 2nd edn (Boston: Academic)
- [20] Rapaport D C 2004 *The Art of Molecular Dynamics Simulation* (Cambridge: Cambridge Academic Press)
- [21] van Zon R 2008 Smoothed potentials for spherical nanoparticles *Preprint arXiv: 0803.4186*[stat-mech]
- [22] Hansen J-P and McDonald I R 1988 *Theory of Simple Liquids* 4th edn (London: Academic)
- [23] Squires G L 1978 *Introduction to the Theory of Neutron Scattering* (Cambridge: Cambridge University Press)
- [24] van Kampen N G 1992 *Stochastic Processes in Physics and Chemistry* (Amsterdam: North-Holland)
- [25] Schofield P 1961 *Inelastic Scattering of Neutrons in Solids and Liquids* (Vienna: International Atomic Energy Agency) p 31
- [26] Sears V F 1972 *Phys. Rev. A* **5** 452–62
- [27] Evans D J and Morriss G P 1990 *Statistical Mechanics of Nonequilibrium Liquids* (London: Academic)
- [28] Yvon J 1943 *Cahiers Physique* **14** 1–17
- [29] van Zon R and Schofield J 2002 *Phys. Rev. E* **65** 011107